Theoretical and experimental comparison of two interoperable dynamic wireless power transfer systems for electric vehicles

Theoretical and Experimental Comparison of Two Interoperable Dynamic Wireless Power Transfer Systems for Electric Vehicles

Riccardo Ruffo, Mojtaba Khalilian, Vincenzo Cirimele and Paolo Guglielmi
Department of Energy, Politecnico di Torino
Torino, Italy
email: name.surname@polito.it

Mario Cesano
Innovative Technologies Dept. – Power Electronics
SAET S.p.A
Leinì, Torino, Italy
email: mario.cesano@saetemmedi.com

***Abstract*—The paper discusses two wireless power transfer systems for the charge of electric vehicles during the motion. The systems are conceived to be interoperable with the same receiver structure. Both systems are supplied by means of the same power electronics architecture and are based on the series-series compensation of the coils. In one of the presented systems a high-frequency transformer is used at the transmitter side. The two solutions are analyzed and compared pointing out their advantages and drawbacks. Results of experimental tests are presented to demonstrate the operations of both systems.**

Keywords—Electric vehicle, dynamic charging, wireless power transfer.

I. INTRODUCTION

Over the past few years, electric vehicles (EVs) have rapidly developed. However, EVs are still affected by the problems of limited range and the need of frequent stops for the charge due to the low energy density of batteries. Furthermore, the weight and the cost of the batteries are other limitations in widespread use of electric vehicles. Dynamic wireless power transfer (WPT) is a possible solution for these issues [1]-[3]. With the dynamic charge, the transmission of the power to the battery is carried out in absence of electrical contacts when the EV is in motion. Thus, the EV range can be extended and the size and weight of the battery can be reduced.

In dynamic WPT systems, the transmitter coils are generally buried in the road while the receiver coil is mounted under the vehicle. Several WPT systems have been introduced in literature at various rated powers [2]–[11]. Generally, two main coil topologies are employed for the transmitters; the long track coil [4]-[6] and the segmented coil [7]-[11]. In long coil topology, the transmitter is much longer than the receiver. This results in a more constant coupling while the vehicle moves along the track. However, the efficiency is low as the magnetic coupling of the coils is typically weak. In segmented coil topology, the length of the transmitter is smaller than the size of the vehicle. Thus, the coupling coefficient is higher in comparison with the long track topology. This results in an improvement of the efficiency. In this topology, a separate converter can be employed for each transmitter coil. The converter can be turned on when the vehicle is above the transmitter coil. Besides the improvement of the efficiency, this will significantly help in reduction of stray field [11]. Another advantage of the segmented topology over long track topology is that the self-inductance of the transmitter coil is considerably smaller meaning a lower voltage stress over the transmitter compensation capacitor. However, since each coil is energizied by a separate H-bridge, in segmented topology, the total cost is higher and the coil circuit is more complicated.

Furthermore, some work has proposed the use of a high-frequency transformer at the transmitter side [12], [13]. The main role of this component is to provide an additional insulation level for the system.

This paper presents two systems, indicated as system A and system B, both based on the segmented transmitter topology and a rectangular shape of transmitter and receiver coils. The two solutions adopt the series-series compensation, but the system B is characterized by the presence of a high-frequency transformer on the transmitter side. The two systems have been developed to operate in the same electrical infrastructure in which each transmitter is supplied by means of a dedicated DC/AC converter and the overall WPT infrastructure is powered through a DC distribution line. Moreover, system B has been designed to be interoperable with respect to the same structure of the receiver developed for the system A.

Solutions A and B are investigated and compared in terms of efficiency and voltage stress over the compensation capacitors focusing also on the aspects of the common mode currents once the transmitters are directly embedded in the road pavement. The comparison is carried out also performing experimental tests.

II. SYSTEM DESCRIPTION

Fig. 1 shows the general architecture of the systems under analysis. Both systems are supplied by a main DC bus provided by an active AC/DC converter. The DC bus powers each WPT section (in the red box in Fig. 1) composed by an H-bridge and its transmitter coil together with the capacitive elements for the compensation. The entire system is directly connected to the LV distribution network through an insulation transformer that electrically separates the system and the normal three-phase distribution line.

On the EV side (in the green box of Fig. 1), the receiver structure is composed of the receiver coil with its compensation capacitor, a diode rectifier and a DC/DC boost converter that acts as interface between the receiver and the battery by regulating the received power. The paper focuses on the content of the red box of Fig. 1. Both systems are supplied

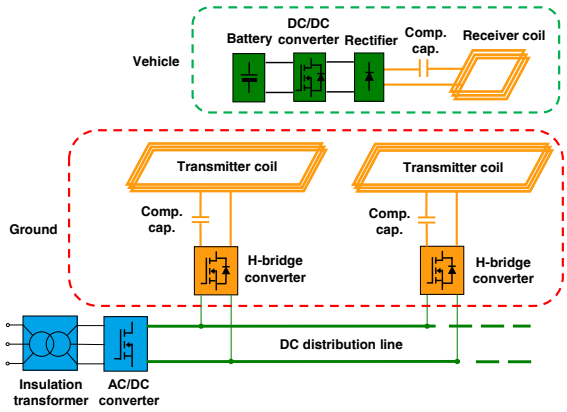

Fig. 1. General architecture of the WPT system infrastructure

by the same H-bridge but the characteristics of the transmitter and the compensation capacitor change according to the insertion of a high-frequency transformer in the solution B. The remaining parts of the infrastructure do not change. Hence, the proposed solutions for the WPT are completely interoperable. The characteristics of each system is presented in the following.

A. System A

The architecture of system A is shown in Fig. 2. L_1 and L_2 are the self-inductance of transmitter and receiver respectively and M represents their mutual inductance. R_1 and R_2 represent the resistances of the coils. The two capacitors C_1 and C_2 are employed in order to improve the power transfer capability of the system [3],[5],[6]. These capacitors are chosen in order to resonate with the self-inductance of the respective coil at a unique common resonance frequency ω_0:

$$\omega_0 = \frac{1}{\sqrt{L_1 C_1}} = \frac{1}{\sqrt{L_2 C_2}} \tag{1}$$

As shown by (1), the series-series compensation topology is chosen because the resonant circuit can be designed independently of the mutual coupling. This is considered an important advantage for the dynamic applications when the mutual coupling naturally varies during the movement of the vehicle.

For both systems the H-bridge operates at fixed frequency ω_0 and the output voltage V_1 is controlled by means of a phase shift modulation. This modulation technique is based on the control of the phase angle α between the gate signals of the two legs of the H-bridge. The relation between the rms value of the first harmonic of V_1 and the angle α is expressed as:

$$V_1 = \frac{2\sqrt{2}}{\pi} V_{in} \cos\left(\frac{\alpha}{2}\right) \tag{2}$$

Where, V_{in} is the amplitude of the DC bus voltage. Fig. 3 shows an example of the waveforms of the gate signals for the switches of the H-bridge and the related output voltage. When α is set to 0°, the maximum converter output voltage can be determined.

Beside the control of the system with the H-bridge converter, a DC/DC boost converter is used on the receiver

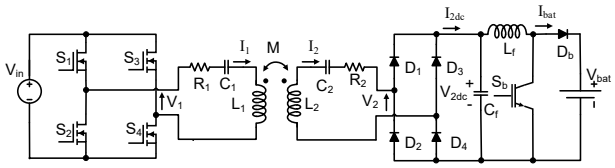

Fig. 2. Power circuit architecture of system A

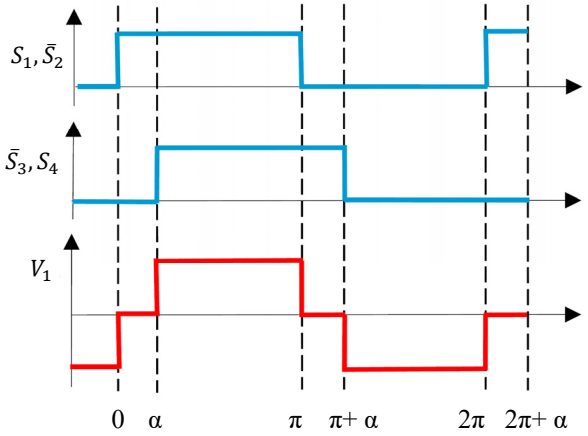

Fig. 3. Gate signals and H-bridge output voltage

side in order to control the voltage V_{2dc} at the output of the diode bridge. The ratio between V_{2dc} and I_{2dc} defines an equivalent resistance. This resistance can be translated on the AC side upstream the diode bridge thanks to a first harmonic approximation:

$$R_{ac} = \frac{8 V_{2dc}}{\pi^2 I_{2dc}} \tag{3}$$

The resistance R_{ac} allows to simplify battery, DC/DC converter and diode-bridge using a single parameter.

If the system works at the resonance frequency, it is possible to express the rms values of transmitter and receiver current as:

$$I_1 = \frac{R_2 + R_{ac}}{R_1(R_2 + R_{ac}) + (\omega_0 M)^2} V_1 \tag{4}$$

$$I_2 = \frac{\omega_0 M}{R_1(R_2 + R_{ac}) + (\omega_0 M)^2} V_1 \tag{5}$$

The power received at the diode bridge input is then defined by the following equation:

$$P_2 = \frac{R_{ac}(\omega_0 M)^2}{[R_1(R_2 + R_{ac}) + (\omega_0 M)^2]^2} V_1^2 \tag{6}$$

Hence the efficiency of the AC section (i.e. the efficiency between the H-bridge output and the diode bridge input) can be expressed as:

$$\eta = \frac{R_{ac}(\omega_0 M)^2}{(R_2 + R_{ac})[R_1(R_2 + R_{ac}) + (\omega_0 M)^2]} \tag{7}$$

Equations (6) and (7) clearly point out as the mutual inductance plays a key role in the power transfer.

It is worth noting that, in the condition of maximum voltage at the H-bridge output and for a given battery voltage, there is only one value of mutual inductance that allows the transfer of a certain power P_2. If losses are neglected, the previous assumption can be viewed in the light of the following equation:

$$M = \frac{8}{\pi^2}\frac{V_{in}V_{bat}}{\omega_0 P_2} \tag{8}$$

B. System B

One of the main critical issues of WPT systems for EVs is represented by the high voltage stress over the compensation capacitors [14]. This voltage can reach the decade of kilovolt for applications whose power rating is in the order of decades of kilowatt. A possible way to mitigate this voltage stress on the transmitter side could be represented by the introduction of a transformer between the H-bridge and the transmitter resonant circuit as shown in Fig. 4.

For the sake of simplicity, the non-idealities of the transformer are neglected. Hence, equations (3), (4), (5), (6) and (7) developed for the system A, can be considered valid also for the system B under the following conditions:

$$I_1 = I_1^{'}N, V_1 = \frac{V_1^{'}}{N} \tag{9}$$

where N is the transformer ratio.

The interoperability between the two systems can be guaranteed only if the transmitter of system B maintains the same amperes/turns ratio of the transmitter of system A. This means that, in order to demand the same voltage and current at the H-bridge output, the number of turns of the transmitter has to be decreased by a factor N. In first approximation, this means a reduction of the transmitter self-inductance by a factor N^2 but also a reduction of the mutual inductance by a factor N [5]. In this case, (8) has to be rewritten by considering this effect:

$$M = \frac{8}{\pi^2}\frac{V_{in}V_{bat}}{\omega_0 P_2}\frac{1}{N} \tag{10}$$

Equation (10) indicates that the power P_2 can be transferred with the same couple of values of V_{in} and V_{bat} used in system A if the mutual inductance is decreased by a factor N. This demonstrates the interoperability of the two systems while maintaining unaltered the receiver section and the characteristics of the transmitter source.

The reduction of the self-inductance L_1 by a factor N^2 leads to a modification of the value of its compensation capacitor in order to maintain the same resonance frequency defined in (1). This means that the capacitance C_1 has to be increased by a factor N^2. By expressing the rms voltage over the capacitor C_1 as

$$\Delta V_{C1} = \frac{I_1}{\omega_0 C_{1sysB}} = \frac{N I_1^{'}}{\omega_0 C_{1sysA} N^2} \tag{11}$$

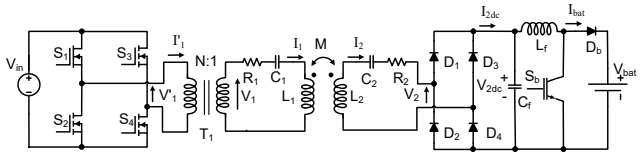

Fig. 4. Power circuit configuration of system B

one can see that, in the systems B, the voltage stress over the capacitor can be reduced by a factor N.

Finally, the introduction of the transformer requires a strong modification of the compensation capacitor parameters. This capacitance strongly increases while the requirements in terms of current become more important and the requirements in terms of tolerated voltage become less critical. From another point of view, the insertion of the transformer can be used as an additional degree of freedom in the design of the WPT system. The transformer ratio N can be chosen to match the characteristics of the compensation capacitor with the characteristics of commercially available capacitors. The developed considerations have been based on the hypothesis of an ideal behavior of the transformer. In real implementations the presence of the leakage inductance L_{lk} of the transformer has to be taken into account in the selection of the capacitors by using the following relationship:

$$C_1 = \frac{1}{(L_{lk} + L_1)\omega_0^{\,2}} \tag{12}$$

III. EXPERIMENTAL RESULTS

A. Test setup description

The physical implementation of system A and system B consists of two WPT systems with a rated power of 20 kW. The systems are supplied by means of a three-phase insulated transformer and an AC/DC providing a DC bus at 600 V. The tests have been conducted by using as load a battery having rated voltage of 300 V. The transmitter is supplied through an H-bridge converter based on a SiC MOSFET module. The H-bridge operates at a fixed frequency equal to 85 kHz with a rated current of 40 A rms. For both system A and system B the distance between transmitter and receiver is maintained fixed at 25 cm. The adopted receiver, equal for the two systems, is shown in Fig. 5. It consists of a rectangular coil made of ten turns of litz wire and two ferrite cores placed in the sides parallel to the direction of movement of the vehicle on which the receiver has to be placed. The parameters of the receiver are presented in TABLE I.

B. System A description

Fig. 6 shows the transmitter coil of system A during the embedding in the road surface. In this implementation, the use of ferromagnetic materials is limited to the receiver only. The parameters of the transmitter of system A are listed in TABLE II.

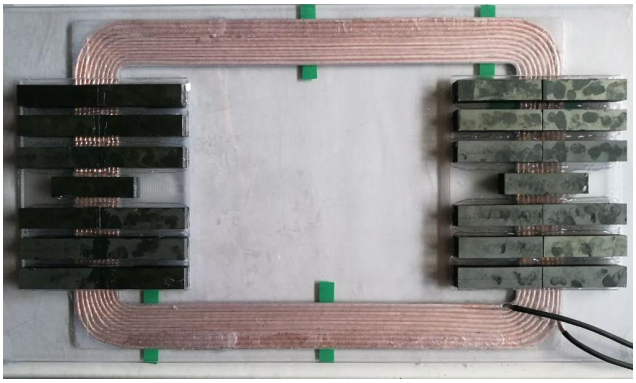

Fig. 5. Structure of the receiver coil

TABLE I.
PARAMETERS OF THE RECEIVER

Parameter	Value	Unit
Receiver resistance, R_2	0.3	Ω
Receiver inductance, L_2	120	µH
Receiver capacitor, C_2	29.2	nF
Receiver coil external length	60	cm
Receiver coil external width	40	cm
Receiver coil number of turns	10	-

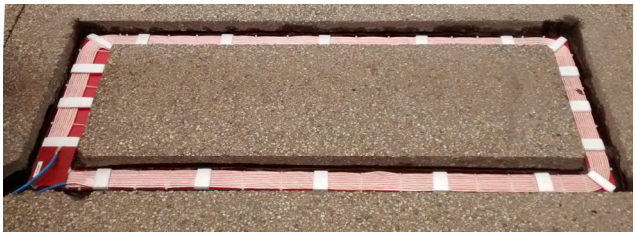

Fig. 6. Structure of the transmitter coil for system A during the embedding in the road surface.

TABLE II.
PARAMETERS OF SYSTEM A

Parameter	Value	Unit
Transmitter resistance, R_1	0.5	Ω
Transmitter inductance, L_1	280	µH
Transmitter capacitor, C_1	12.5	nF
Mutual inductance, M	14.3	µH
Transmitter coil length	150	cm
Transmitter coil width	50	cm
Transmitter coil number of turns	10	-
Wire diameter	5	mm

C. System B description

The transmitter coil adopted in system B is shown in Fig. 7. In this case, the transmitter is constituted by a single-turn coil with an increased diameter of the wire to tolerate the increased value of the current.

As shown in Fig. 8, a high-frequency transformer with transformer ratio N=10 is inserted between the H-bridge and the compensation capacitors. In the physical implementation these components are placed in the same case. The overall value of capacitance equal to 600nF is made by using five capacitors of 500nF i.e. the parallel of three capacitors in series with the parallel of two capacitors. With respect to system A,

Fig. 7. Structure of the transmitter coil for system B during the embedding in the road surface.

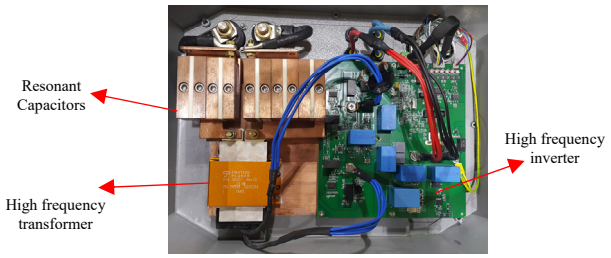

Fig. 8. Power electronics structure of the System B. Transmitter converter, transformer and capacitors.

TABLE III.
PARAMETERS OF SYSTEM B

Parameter	Value	Unit
Transmitter resistance, R_1	8.6	mΩ
Transmitter inductance, L_1	5.2	µH
Transmitter capacitor, C_1	600	nF
Transmitter coil length	200	cm
Transmitter coil width	58	cm
Mutual inductance, M	1.7	µH
Transmitter coil number of turns	1	-
Wire diameter	10	mm
Transformer turn ratio, N	10	-
Transformer leakage inductance referred to low voltage side, L_{lk}	0.55	µH
Transformer magnetizing inductance	2.85	mH

the length of the transmitter has been slightly increased in order to tune the resonance frequency at a value as close as possible to 85 kHz. The main parameters of the transmitter of system B are presented in TABLE III.

It is worth nothing that the change of wire diameter and length of the transmitter coil do not allow the scaling of the self-inductance by a factor N^2. Conversely these changes have a less significant effect on the mutual inductance that is reduced by a factor 8.4.

D. Experimental comparison

Firstly, the two systems have been tested at the same power level of 10 kW at the H-bridge output for a passage of the receiver at a limited speed of about 4 km/h. The related waveforms are shown in Fig. 9 and Fig. 10.

As visible in these figures, the waveforms of the transmitter voltage are different in the two cases. This difference is due to the fact that the mutual inductance of system B is not scaled by a factor N with respect to the mutual inductance of system A. In the case of system B, the value of M is proportionally higher than the value of system A. According to (10) this means that

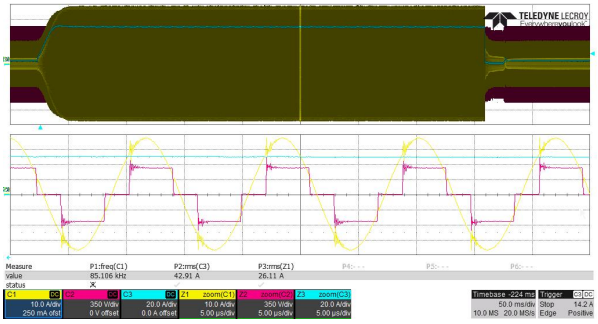

Fig. 9. System A waveforms. Top: transmitter current in yellow (10 A/div), transmitter voltage in red (350 V/div) and receiver DC current in blue (20 A/div). Bottom: zoomed waveforms.

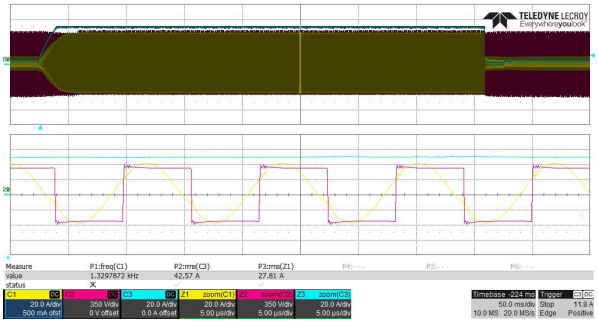

Fig. 10. System B waveforms. Top: transmitter current in yellow (20 A/div), transmitter voltage in red (350 V/div) and receiver DC current in blue (20 A/div). Bottom: zoomed waveforms.

system B requires a slightly higher voltage to transfer the same power.

A second series of tests have been carried out to evaluate the aspects of the ground currents (i.e. the common mode currents that can flow from the embedded coils and cables through the ground by means of capacitive coupling). These currents can represent a problem when a complete WPT charging lane is active and many converters switch together in close spatial proximity. In such cases the ground current could cause EMC problems with respect to the auxiliary electronics for the communications and the management of the charging process [15].

Ground currents for both systems have been measured as the sum of the phase currents at the output of the insulated three-phase transformer that supplies the system. As could be seen in Fig. 11 and Fig. 12, a ground current takes place in correspondence of the H-bridge commutations. The peak of the ground current is not the same for the two systems. The current peak reaches 1A for system A while a value of 500 mA is measured for system B. This difference can be ascribed to two factors:

1. The reduced number of turns of the transmitter coil of system B. This means a reduced surface of the coil thus a reduction of the capacitive coupling with respect to the ground
2. The presence of the high-frequency transformer that provides an additional level of electrical insulation between coil and source.

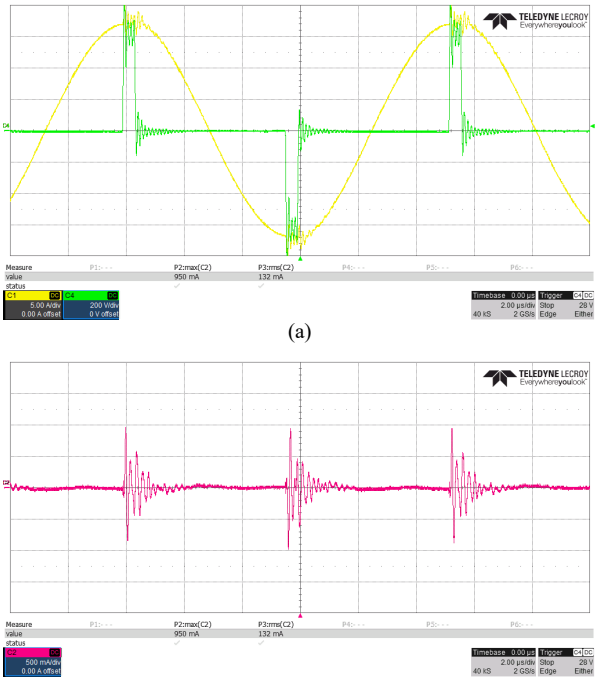

(a)

(b)

Fig. 11. System one waveforms. (a) Transmitter current in yellow (5 A/div) and voltage in green (200 V/div). (b) Ground current in red (500 mA/div).

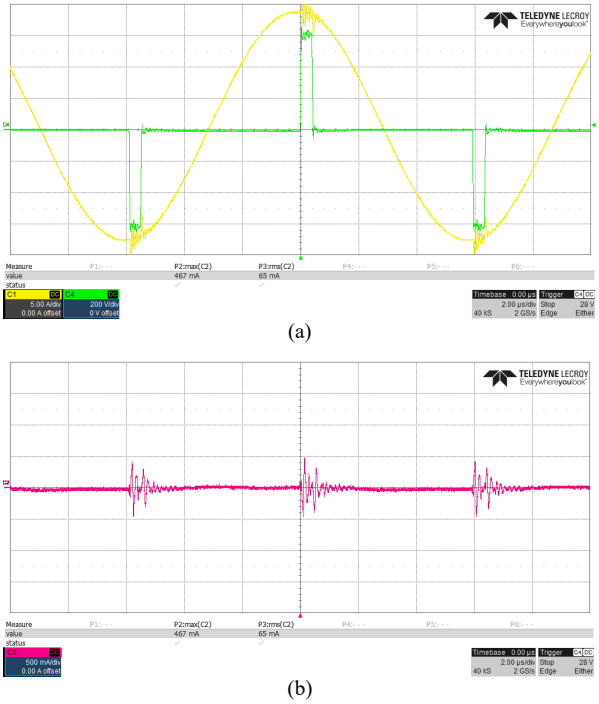

(a)

(b)

Fig. 12. System two waveforms. (a) Transmitter current in yellow (5 A/div) and voltage in green (200 V/div). (b) Ground current in red (500 mA/div).

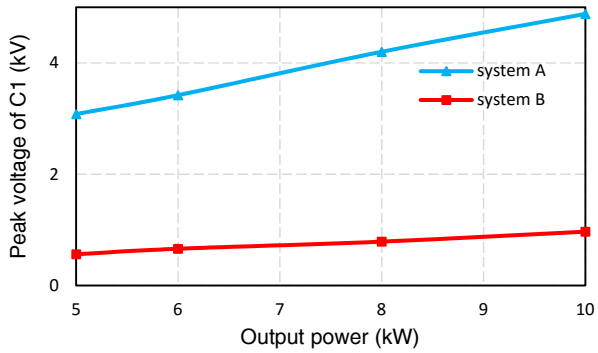

Fig. 13. Capacitor voltage versus output power.

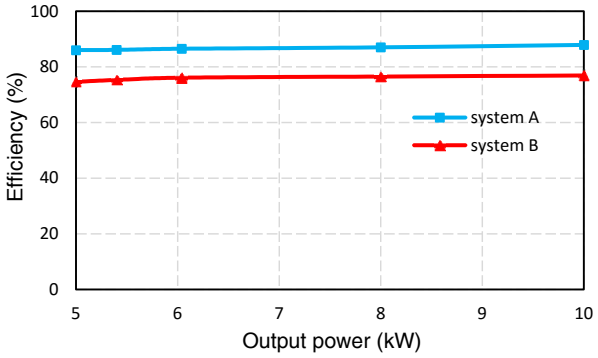

Fig. 14. Efficiency comparison between two systems versus output power.

The effect of the voltage stress of the compensation capacitors is presented through Fig. 13. This figure shows the voltage over the compensation capacitors for different powers measured at the H-bridge output. As expected, the voltage stress over the capacitor of system B is strongly reduced to about one fifth of the voltage of the capacitor of system A.

Finally, the comparison of the DC-to-DC efficiency of the two systems for different powers is shown in Fig. 14. At the supplied power of 10 kW, the efficiency of system B is 76.9% and the efficiency of the system A is 87.9%. This difference of efficiency is due to the additional losses introduced by the high-frequency transformer.

IV. Conclusion

The carried out comparison has pointed out several differences between the analyzed systems. The origin of these differences is mainly due to the use of the high-frequency transformer as interface between the power electronics powering the system and the resonant transmitter section. The presence of the transformer has introduced two strong benefits that are the reduction of the ground currents and the reduction of the voltage stress over the compensation capacitor. However, this component causes an increase in the cost of the solution and a relevant decrease of the system efficiency.

Acknowledgment

This work has been co-funded by the European Union's 7th Framework Program for Research through the FABRIC project (No. FP7 605405). Also, the authors would like to thank SAET Company for contribution to this work.

References

[1] L. Zhao, S. Ruddell, D. Thrimawithana, U. K. Madawala, P. A Hu, "A hybrid wireless charging system with DDQ pads for dynamic charging of EVs," *in Proc. of IEEE 2017 WOW Conf.*, 2017.

[2] S. Li and C. C. Mi, "Wireless power transfer for electric vehicle applications," *IEEE Journal of Emerging and Selected Topics in Power Electronics*, vol. 3, no. 1, pp.4–17, 2015.

[3] V. Cirimele, F. Freschi and M. Mitolo, "Inductive power transfer for automotive applications: State-of-the-art and future trends," *IEEE Industry Applications Society Annual Meeting*, pp. 1-8, 2016.

[4] M. L. G. Kissin, G. A. Covic, and J. T. Boys, "Steady-state flat-pickup loading effects in polyphase inductive power transfer systems," *IEEE Trans. on Ind. Elec.* , vol. 58, pp. 2274–2282, June 2011.

[5] J. Huh, S. W. Lee, W. Y. Lee, G. H. Cho, and C. T. Rim, "Narrow-width inductive power transfer system for online electrical vehicles," *IEEE Transactions on Power Electronics*, vol. 26, pp. 3666–3679, Dec 2011.

[6] S. Y. Choi, B. W. Gu, S. Y. Jeong and C. T. Rim, "Advances in wireless power transfer systems for roadway-powered electric vehicles," *IEEE J. Emerg. Select. Topics Power Electron.*, vol. 3, no. 1, pp.18–36, 2015.

[7] M. Yilmaz, V. T. Buyukdegirmenci, and P. T. Krein, "General design requirements and analysis of roadbed inductive power transfer system for dynamic electric vehicle charging," *in 2012 IEEE Transportation Electrification Conference and Expo (ITEC)*, pp. 1–6, June 2012.

[8] S.G. Rosu, M. Khalilian, V. Cirimele, P. Guglielmi, "A dynamic wireless charging system for electric vehicles based on DC/AC converters with SiC MOSFET-IGBT switches and resonant gate-drive," *in Proc. of IEEE IECON Conf.*, 4465–4470, 2016.

[9] G. Buja, M. Bertoluzzo, and H. K. Dashora, "Lumped track layout design for dynamic wireless charging of electric vehicles," *IEEE Trans. Ind. Electron.* , vol. 63, no. 10, pp. 6631–6640, Oct. 2016.

[10] F. Lu, H. Zhang, H. Hofmann, and C. C. Mi, "A dynamic charging system with reduced output power pulsation for electric vehicles," *IEEE Transactions on Industrial Electronics*, vol. 63, pp. 6580-6590, 2016.

[11] V. Cirimele, P. L. Pichon, F. Freschi, "Electromagnetic modeling and performance comparison of different pad-to-pad length ratio for dynamic inductive power transfer," *in Proc. of IEEE IECON Conf.*, 4499–4503, 2016.

[12] J. Miller, O. Onar, and M. Chinthavali, "Primary-side power flow control of wireless power transfer for electric vehicle charging," *IEEE J. Emerg. Sel. Topics Power Electron.* , vol. 3, no. 1, pp. 147–162, Mar. 2015.

[13] M. Chinthavali, Z. Wang, S. Campbell, "Analytical modeling of wireless power transfer (WPT) systems for electric vehicle application," *in Proc. of IEEE ITEC Conf.*, 2016.

[14] J. Shin *et al.*, "Design and implementation of shaped magnetic-resonance-based wireless power transfer system for roadway-powered moving electric vehicles," *IEEE Trans. Ind. Electron.*, vol. 61, no. 3, pp. 1179–1192, Mar. 2014.

[15] R. Ruffo, and P. Guglielmi, "Simple parameters estimation and precise over-voltage simulation in long cable connected drives," In *Industrial Electronics Society, IECON 2016-42nd Annual Conference of the IEEE*, pp. 4362-4367, 2016.